



## ORIGINAL RESEARCH

# The Low Emission Oil and Gas Open reference platform—An off-grid energy system for renewable integration studies

Harald G. Svendsen | Til Kristian Vrana | Andrzej Holdyk | Heiner Schümann

SINTEF, Trondheim, Norway

**Correspondence**Harald G. Svendsen, SINTEF, Trondheim, Norway.  
Email: [harald.svendsen@sintef.no](mailto:harald.svendsen@sintef.no)**Funding information**Norges Forskningsråd, Grant/Award Number:  
296207**Abstract**

This article introduces and describes the integrated energy system of the Low Emission Oil and Gas Open reference platform. It is a hypothetical case meant to represent a typical oil and gas installation in the North Sea. The aim of this detailed specification is to serve as an open reference case where all the information about it can be publicly shared, facilitating benchmarking and collaboration. The relevance of this reference case of an off-grid energy system is not limited to the oil and gas industry, since it can also be seen as a special kind of electrical micro grid. The remote offshore location makes it especially relevant for studying offshore wind power and ocean energy sources like wave power. The specification has an emphasis on the energy system and electrical configuration, but also includes a basic description of the oil field and processing system. The intention is that it will serve as a basis for energy system studies and relating power system stability analyses regarding the integration of renewable energy sources. This allows for comparisons of a base case with different design modifications, new operational planning methods, power management strategies and control concepts. Examples of possible modifications are the replacement of gas turbines by wind turbines, addition of energy storage systems, a more variable operation of loads etc. The last part of the article demonstrates the behaviour of the reference platform implemented in two software tools: one for operational planning and one for dynamic power system analyses.

**KEYWORDS**

energy management systems, power generation control, power system simulation, power system stability, smart power grids

## 1 | INTRODUCTION

To eliminate or reduce CO<sub>2</sub> emissions from the local energy system at offshore oil and gas platforms, fossil-fuel based gas turbines must either be equipped with carbon capture and storage technologies [1] or be replaced by clean alternatives such as power from offshore wind turbines, power via cable from shore, a shift to hydrogen-based gas turbine fuels or fuel cells, power from other renewable sources, or other solutions that eliminate emissions. With new energy supply alternatives, new operating strategies are required in order to best utilise the available resources within the given constraints. And the new technology will have different electrical characteristics that must be addressed. To demonstrate the adequacy and benefit

of new low-emission solutions, new models and methods are needed to analyse the system operation and to show that the energy supply system can provide the required security of supply and power system stability.

### 1.1 | LEOGO reference platform

To more easily demonstrate and test new operating strategies, different system configurations, control concepts and new ideas and methods for integrating renewables into an off-grid system, it is useful to have an open and well-defined test case as a common basis for analyses. Therefore, we have created what we call the *Low Emission Oil and Gas Open* (LEOGO)

This is an open access article under the terms of the Creative Commons Attribution License, which permits use, distribution and reproduction in any medium, provided the original work is properly cited.

© 2022 The Authors. *IET Energy Systems Integration* published by John Wiley & Sons Ltd on behalf of The Institution of Engineering and Technology and Tianjin University.

reference platform. It is intended as a well-defined study case where all the underlying data can be publicly shared. It constitutes both a *specification* and a *dataset* that is publicly available [2].

This work has been done within the *Low-Emission* research centre, which is a collaboration between the research and industry partners that are aiming to develop technology to reduce emissions from petroleum activities on the Norwegian continental shelf (NCS). The LEOGO specification has been created with crucial input from industry partners in this centre.

Real oil and gas platforms of course differ from each other in important ways and analyses of this reference platform can never substitute case-specific analyses. But often, especially in early phases of development, it is interesting to explore ideas in a general context without a specific case in mind. And from a research perspective, the main interest is often the demonstration of generic concepts where the peculiarities of the study case are less important. Hence we believe that a completely open and freely available case specification can prove useful both for academic research and for industry development.

When required for a particular purpose, the reference case presented here may be adjusted. In such cases, we would encourage authors to indicate very clearly what modifications have been made when reporting their results.

The LEOGO specification in its present form is primarily concerned with the energy system and its links with the topside processing system. Details regarding reservoir and fluid transport from the reservoir to the platform is not included: The boundary is taken to be the flow and pressure at the separator inlet. Even with this limited scope, it is inevitable that every detail is not described in this specification. Additional information on general relevance may be added in future updates.

## 1.2 | Literature

Offshore energy systems and solutions for CO<sub>2</sub> emission reduction from oil and gas platforms is a topic that has been addressed and analysed in several studies in the literature [3–8], and several of these consider Norwegian offshore oil and gas platforms. However, the cases and the assumptions are not documented in detail, making it difficult to test their conclusions and compare their results. Lack of documentation may be due to confidentiality issues when working with real cases and data obtained from the industry, or it may be that even though the full data in principle is open, the studies only describe the subset of the data that is directly relevant for the discussion in the given study.

Although we are not aware of any open datasets of a similar scope to what we present here, a lot of oil and gas data is openly available, notably historical production data made it available through the Norwegian Petroleum Directorate's data repository [9]. Several open reservoir models [10] that are relevant for analyses of subsurface dynamics also exist. A general description of offshore processing systems and configurations can be found in Ref. [11]. However, for the exact

modelling of power consumption, detailed information is necessary regarding produced fluid properties, export conditions and processing unit set points and performance. Still, such details are normally not available due to confidentiality. Some examples of modelled processing facilities and associated power consumption can be found in Refs. [5, 12–15]. Some electrical data and diagrams from real North Sea platforms have been published [16], but again the description is incomplete and the underlying data are not provided.

## 1.3 | Contributions

The main contribution of this article is the specification of a realistic and open reference oil and gas platform as a suitable study case that facilitates reproduction and comparison of results obtained with different methods and tools. Additionally, actual implementations of this case in two different modelling environments are presented together with basic simulation results that show the platform in operation including some of its electrical characteristics. More thorough analyses are left for future publications.

## 2 | GENERAL SPECIFICATIONS

The LEOGO reference platform is meant to be representative of what could be considered a typical oil and gas platform on the Norwegian Continental Shelf (NCS), with oil and gas production rates being compared to other fields as indicated in Figure 1. Although a hypothetical field and platform, its characteristics have been chosen to be *realistic* in the sense that it *could have been* a real platform: The gas over oil ratio and fluid pressure levels is typical for platforms in the North Sea. The LEOGO platform is considered to be in plateau production phase, with oil, gas and water extraction rates that are comparable to several other large fields. The platform's electric power demand of about 47 MW matches these assumptions. The electricity and heat supply is from local gas turbines of the type most commonly found on the NCS. All compressors and pumps are electric, which is typical for new installations. For older installations, large compressors and pumps are more often mechanically driven directly by gas turbine shafts. The choice of assuming electric machinery is partly because it is more common for new installations and partly because it offers better control and is thus more interesting for a study case.

The specification has a strong emphasis on the energy system and on what is relevant for energy system operational planning, power management and electrical stability, considering timescales of a month down to milliseconds. Reservoir dynamics and long-term changes in production rates and resulting changes in energy demand are not included.

The electrical grid can be considered as a type of micro grid. However, some characteristics make it different from most other micro grid systems. Firstly, the power consumption is dominated by large motors, with and without variable speed

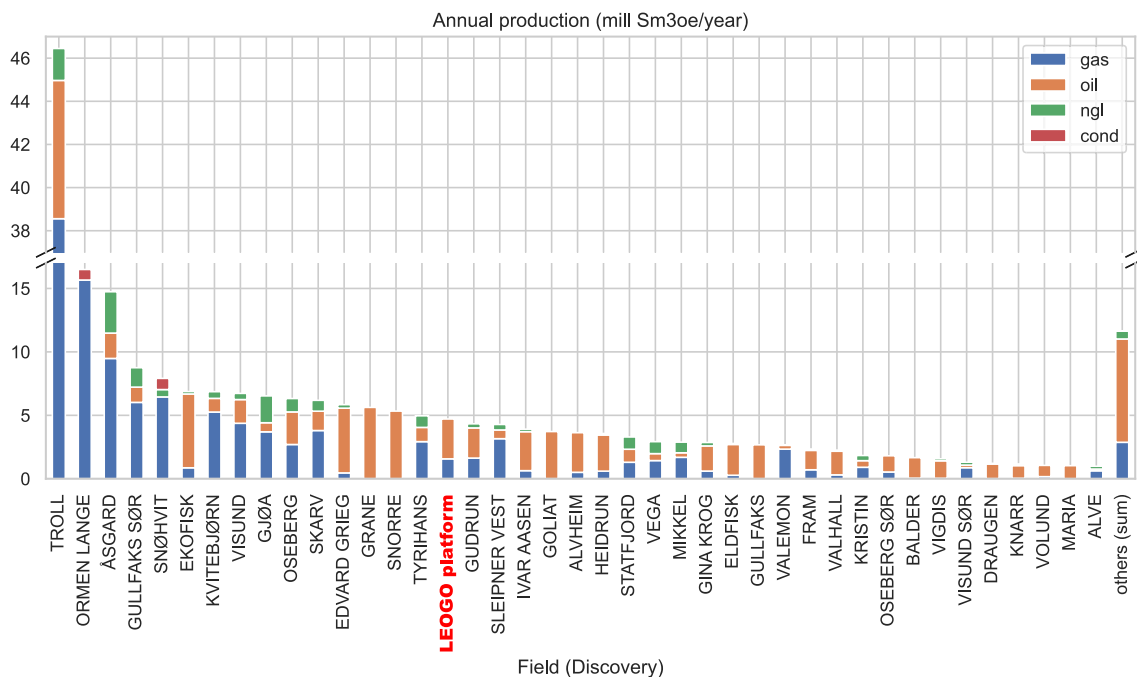


**FIGURE 1** Low Emission Oil and Gas Open (LEOGO) reference platform compared to Norwegian continental shelf platforms in 2018 in terms of production of natural gas, oil, natural gas liquids (ngl) and condensate (cond). (data source: Norwegian Petroleum Directorate)

drives. Secondly, the power supply from gas turbine generators of this size range, in combination with wind turbines. And finally, the grid itself with its voltage levels and short cable distances.

This specification may be updated and expanded in the future as needed. For example, to make the case relevant for lifetime analyses and investment optimisation, energy demand variations over many years are needed.

A schematic of the platform's processing and energy system is shown in Figure 2, with details described in the following.

## 2.1 | Oil field and processing characteristics

The LEOGO case represents an oil and gas field with the main characteristics as shown in Table 1. The platform processes petroleum from multiple production wells, and the wellstream transport from the reservoirs up to the platform is assisted by gas lift. Gas lift is used instead of electric pumps since it is more common on Norwegian fields. The wellstream pressure at the separator inlet is 2 MPa, as indicated in Figure 2. The reservoir pressure is maintained via water injection, using both water separated out from the wellstream, and additional seawater.

All compressors on the LEOGO platform have electric drives, which is usually the case for modern platforms. On many real older platforms, however, compressors are driven directly by gas turbines, making it more complicated to switch to another energy source than natural gas. The choice of having only electric drives is motivated by the fact that this

allows more easily for a shift of the primary energy source from fossil fuel to renewables, which is the underlying motivation for this work. So either the LEOGO platform may be viewed as a relatively modern installation, or as an older one where the directly-driven compressors have been replaced by electrically driven ones (even though this is an expensive modification).

Separation and gas recompression occurs in three stages. These are integrated processes although they are illustrated with separate blocks in Figure 2 for simplicity.

The electricity demand on the platform is dominated by gas compressors and water injection pumps. Note that some of the compressed gas is re-circulated into the well and used for gas lift. The electricity and heat demand for utility and accommodation can be considered as independent from the production rates. The main heat demand is otherwise in the separation process. Heat is provided via a waste heat recovery from the gas turbines. Flow rates and pressure levels are specified in Figure 2. All flow rates are given as volumetric flow at standard conditions ( $\text{Sm}^3/\text{s}$ ), where standard conditions are  $15^\circ\text{C}$  and normal atmospheric pressure, 101.325 kPa.

The characteristics for oil, natural gas and water fluids are shown in Table 2. Gas gravity, compressibility and temperature are needed to compute pressure drop in gas pipelines by using the Weymouth formula. The specific heat ratio and individual gas constant are relevant for computing the energy demand by compressors. The Darcy friction factors are used to compute pressure drop in pipelines when using the Darcy–Weissbach formula for liquid flow. In reality this factor is not a constant, but dependent on other factors (such as viscosity). The pipeline pressure drop due to friction is especially relevant for



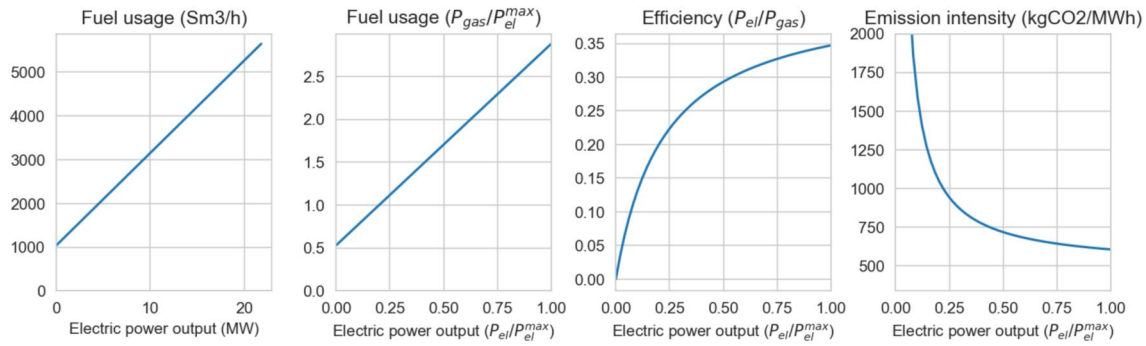


**FIGURE 3** Gas turbine generator fuel usage, efficiency and emission intensity versus power output,  $P_{el}$ .  $P_{gas}$  is the energy content of the gas fuel, and  $P_{el}^{max}$  is the generator capacity.

### 2.3 | Operating state

The operating state will vary over time, and changes in one place will affect other parts, for example, a change in oil and gas production rate will change the power demand in pumps and compressors. Here we specify a *baseline* operating state that may be considered a snapshot at a particular time. For this situation, the electricity supply and demand by different main components is shown in Table 4. The difference between load and generation are mainly electrical losses of the cables, transformers and converters. A small part of the deviation stems from the voltage-dependence of the loads, which means that the loads slightly change their power consumption when the real voltage is not exactly the rated voltage.

Fluid and energy flow rates are indicated in Figure 2. The relationship between flow rates, pressure levels and power demand by pumps and compressors has been computed assuming the water pump efficiency of 0.75, oil pump efficiency of 0.6 and compressor efficiency of 0.75. These relationships are elaborated in Section 2.4. With the high loading of gas compressors, the operating state may be considered to represent the early plateau production phase with a high production rate.

In this operating situation, two gas turbines could be just enough to cover the electricity demand, but the 5 MW reserve requirement means that all three gas turbines are required to be online in normal operation. The total heat demand is 8 MW and is covered by waste heat recovery from the gas turbines, see Table 5.

### 2.4 | Compressor and pump power demand

The pump power demand  $P_{pump}$  can be computed according to the relationship

$$P_{pump} = \frac{1}{\eta} q \Delta p, \quad (1)$$

where  $\eta$  is the efficiency,  $q$  is the flow rate and  $\Delta p = p_2 - p_1$  is the inlet/outlet pressure difference. For the water injection pumps with  $\Delta p = (25-0.7)$  MPa,  $q = 0.277 \text{ Sm}^3/\text{s}$  and  $\eta = 0.75$

this gives  $P_{pump} = 8.97$  MW. Similarly, for the oil export pumps with  $\Delta p = (5-0.3)$  MPa,  $q = 0.098 \text{ Sm}^3/\text{s}$  and  $\eta = 0.6$  it gives  $P_{pump} = 0.79$  MW.

The gas compressor power demand  $P_{comp}$  is computed assuming an adiabatic process and ideal gas, with the equation

$$P_{comp} = \frac{1}{\eta} \frac{k}{k-1} \rho Z R T q \left[ \left( \frac{p_2}{p_1} \right)^a - 1 \right], \quad (2)$$

where  $\rho = 0.8$  is the natural gas density,  $Z = 0.9$  is the gas compressibility,  $R = 500 \text{ J/kg K}$  is the individual gas constant,  $T = 300 \text{ K}$  is the inlet temperature,  $k = 1.27$  is the gas specific heat ratio and  $a = \frac{k-1}{k}$ . For the main gas export compressors with  $\eta = 0.75$ ,  $p_1 = 2$  MPa,  $p_2 = 20$  MPa and  $q = 68 \text{ Sm}^3/\text{s}$  this gives  $P_{comp} = 29.1$  MW.

For the gas re-compression in the separator train, we determine the power demand by assuming a single separation stage and intermediate gas pressure of  $p_1 = 1.4$  MPa. With an outlet pressure of  $p_2 = 2$  MPa we find using the same formula as a power consumption of  $P_{comp} = 3.8$  MW.

Note that several simplifications are made here: In a real system, usually the separation train consists of several separators at different pressure levels and so does the re-compression train. Consequently, the gas rates leaving each separator stage and following gas rates per compressor stage will be different. Most free gas, including lift gas which mainly consists of light components, leaves the separation train in the first stage at higher pressure. The pressure for the oil, however, will be reduced to almost atmospheric conditions in order to remove the remaining gas. Efficiencies for pump and compressor systems will also depend on the system configuration and ability to control these units. These assumptions will lead to some deviation from a real system, which should be acceptable at this point where the focus is on the electrical part.

### 2.5 | Time-series data

The variability in the total wellstream flow rate (production rate) and hence the energy demand as well as the variability in wind power availability are given by time-series data. Data

Description	Capacity (MW)	Loading (MW)
Sea water lift pump 1 (SWL1)	0.75	0.45
Sea water lift pump 2 (SWL2)	0.75	0 (off)
Sea water lift pump 3 (SWL3)	0.75	0 (off)
Air compressor 1 (ACO1)	1.3	0.5
Air compressor 2 (ACO2)	1.3	0.5
Gas export compressor train 1 (GEX1)	10	9.7
Gas export compressor train 2 (GEX2)	10	9.7
Gas export compressor train 3 (GEX3)	10	9.7
Oil export pump 1 (OEX1)	1.5	0.39
Oil export pump 2 (OEX2)	1.5	0.39
Water injection pump 1 (WIN1)	4.8	3.0
Water injection pump 2 (WIN2)	4.8	3.0
Water injection pump 3 (WIN3)	4.8	3.0
Gas re-compressor train (REC)	4.8	3.8
Utility ASM 690 V A (ASM1)	0.25	0.2
Utility ASM 690 V B (ASM2)	0.25	0.2
Utility load 690 V A (LOD1)	2.75	1.05
Utility load 690 V B (LOD2)	2.75	1.05
Utility load 400 V A (LOD3)	0.5	0.25
Utility load 400 V B (LOD4)	0.5	0.25
Drill 1 (DRL1)	0.8	0 (off)
Drill 2 (DRL2)	0.8	0 (off)
Drill 3 (DRL3)	0.8	0 (off)
Drill 4 (DRL4)	0.8	0 (off)
Drill 5 (DRL5)	0.8	0 (off)
Drill 6 (DRL6)	0.8	0 (off)
Consumption deviation		0.12
Converter, transformer and line losses		0.90
SUM electric power demand		48.15
Gas turbine 1	21.8	16.05
Gas turbine 2	21.8	16.05
Gas turbine 3	21.8	16.05
Gas turbine 4	21.8	0 (off)
Wind turbine 1	8.0	0 (off)
Wind turbine 2	8.0	0 (off)
Wind turbine 3	8.0	0 (off)
SUM electric power supply		48.15

**TABLE 4** Electric power capacities and base case loading

provided with the LEOGO specification [2] includes time-series with 1-month duration and 1 min resolution.

For the flow rate/energy demand, the wellstream flow variation is set such that the power demand by compressors

and pumps, following a linear dependency on the flow rate, varies  $\pm 4\%$  with a period of about 25 min. This is based on the inspection of power data from a real case platform. Such power variations are not a generic characteristic, but highly

dependent on the specific case and the type of activities and equipment in use. They are nevertheless included in the present dataset to have some reasonable flow and power demand variation without being concerned about their origin. We consider this acceptable as studies based on this platform specification are likely to be mainly concerned with the energy system and not the processing system. If the processing system is not represented in the model, which is the case only for an electric model, the implementation of the variability is that the energy demand in pumps and compressors vary according to the same time series.

Wind power data has been obtained from the publicly available met mast measurements from Sulafjorden at the coast of Norway [21]. Measurements used are wind speeds at a height of 92.5 m with a resolution of 10 measurements per second (10 Hz sample rate). A coastal fjord location is not fully representative of offshore conditions, with higher levels of turbulence and variation, but is used for lack of better high-resolution wind data that is publicly available and relevant for North Sea locations.

Wind forecasts with a 30 min resolution have been synthetically created by re-sampling the wind speed measurements and then adding random noise to represent the forecast error. This results in a root mean square error (RMSE) deviation of 3.3 m/s between the forecast and actual wind speeds at a resolution of 1 min. Wind power has been computed using the power curve of a real 8 MW offshore wind turbine. The wind speed measurement data and calculated wind power data for

March and April 2020, down-sampled to a 1 min resolution, are included with the LEGO dataset and used in the simulations reported here.

An extract of the time series is shown in Figure 4. The figure shows three curves: The ‘oilgas’ curve represents the wellstream flow rate from the well, which determines the oil/gas production rate and influences power demand in pumps and compressors. The ‘curve\_wind’ profile represents a forecast of the available wind power. The ‘curve\_wind (nowcast)’ profile represents an updated forecast that is available and closer to real-time with less forecast error. In actual operation, there will be some deviations from these forecasts. The two time series for wind are provided to account for the fact that forecasts are regularly updated, and that the wind forecast looking 10 min ahead is less uncertain than the one looking further ahead. The use of two static time series as provided here is a simplification of how regularly updated forecasts would be treated in real-time energy management systems. How different prediction methods can affect system operation is an interesting topic for research that may be pursued using the LEGO platform as a study case.

## 2.6 | Operating strategy

The use of resources and the performance of the system in operation depends on the operational planning strategies and controls. Here, we provide the basic high-level principles. Electrical components (see also Section 3) are controlled in standard ways with typical parameter values. The details about these are included in the model [2] itself.

The baseline operating principles are:

- Oil and gas export is maximised, but limited by the well-stream inflow
- If present, wind turbines are favoured before gas turbines
- Wind power can be curtailed and has an upper value that depends on the wind
- A load shedding scheme will ensure frequency stability in case of a sudden generator failure or similar. It is a last-resort action to maintain stability. (Further details are not yet specified)

**TABLE 5** Heat supply and demand

Description	Loading (MW)
Separation/processing	5.0
Utility and accomodation	3.0
SUM heat demand	8.0
Gas turbine 1	16.3
Gas turbine 2	16.3
Gas turbine 3	16.3
SUM heat supply	48.1

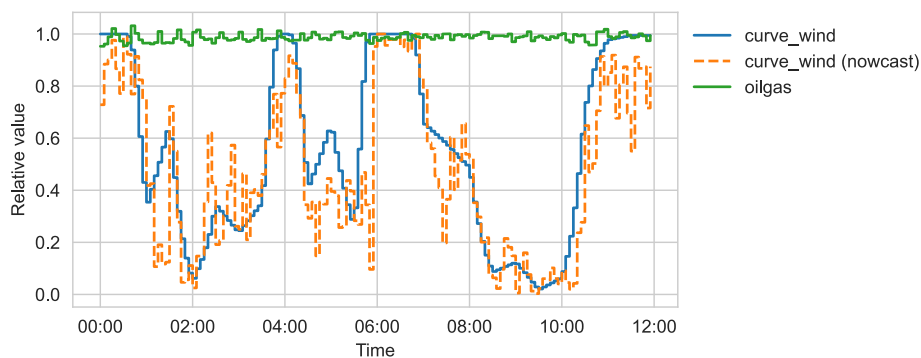


**FIGURE 4** Normalised profiles. The figure shows a 12 h extract of the data, with 5 min resolution.

Important operating constraints are:

- All electricity and heat demand must be met, that is, there is no demand flexibility.
- Minimum 5 MW online (spinning) reserve
- Oil and gas pressure at export points have fixed values
- Water injection rate and pressure are fixed
- 30 minutes startup delay for gas turbine generators

### 3 | ELECTRICAL SYSTEM

In this section, the electrical system is described. This system, although naturally showing some similarities with other (onshore) micro-grids, is composed of generation, load and grid assets typically found on offshore platforms. Unlike many micro-grids, the LEOGO grid is always isolated, and does not have the opportunity to switch between the grid-connected and island mode.

A full description of the electrical system requires a lot of detail regarding the properties of cables and transformers making up the electrical grid and the properties of loads and generators connected to it. For the analyses of a dynamic behaviour, generator control systems play an important role. The same is true for the control systems of other active components, such as variable speed drives for pumps and compressors. In the following, an overview of the various components in the electrical system is given. The system has been modelled in DIgSILENT PowerFactory, and this freely available model [2] includes further details that are not given

here. A simplified single-line diagram of the electrical model is presented in Figure 5.

#### 3.1 | Voltage levels

The platform has four AC voltage levels and one DC voltage level:

- 33 kV<sub>AC</sub> is the voltage that is used for the collection grid of the wind turbines and the transmission to the platform.
- 11 kV<sub>AC</sub> is the voltage at the main busbar system. The gas turbine generators and several of the large loads are connected either directly or via dedicated transformers to this busbar system.
- 690 V<sub>AC</sub> is used for the utility busbar system, where smaller pumps and compressors and auxiliary equipment are connected. It is fed from the 11 kV system via transformers.
- 400 V<sub>AC</sub> is the common low voltage level, and it is used here mainly for the accommodation facilities. The 400 V system is fed from the 690 V system via transformers.
- +1300 V<sub>DC</sub> is used in addition to the AC voltage levels, where a drilling switchboard is operated at this voltage level. This DC busbar system is fed through active power converters in the rectifier mode that connects via the converter transformers to the 11 kV system. The DC system is monopolar, and the return path is through the Earth.

The 11 kV, 690 V and +1300 V<sub>DC</sub> busbar systems are realised as split single busbars with a tie breaker. The 33 kV<sub>AC</sub>

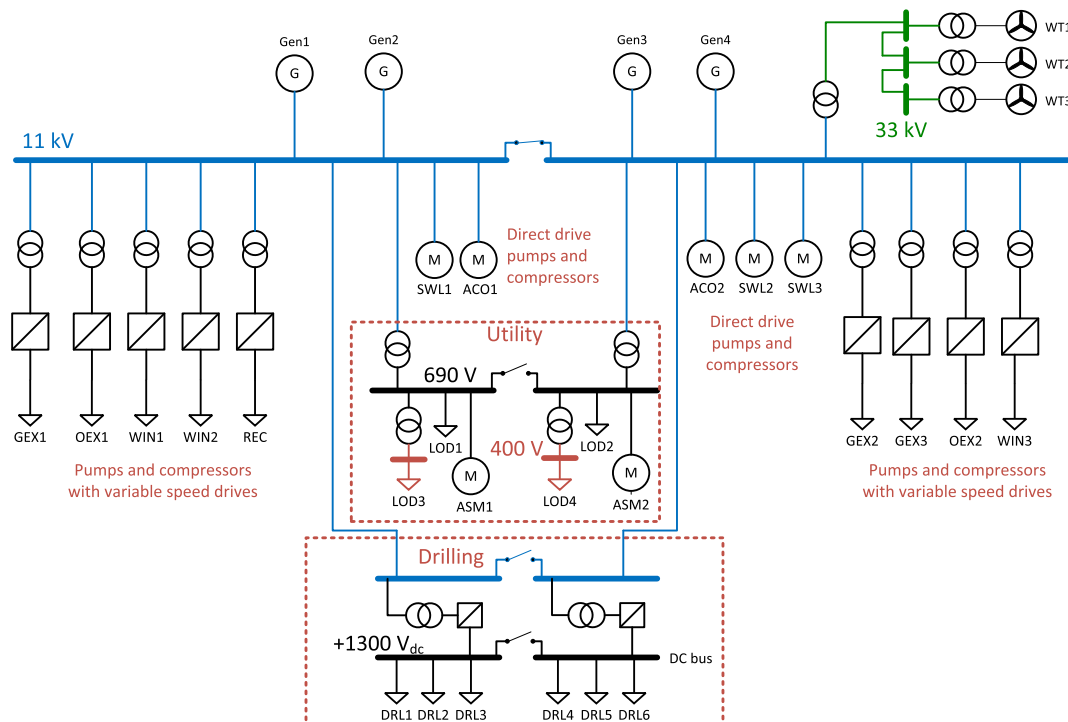


FIGURE 5 Electrical model.

is realised with simple single busbars. The 400 V level consists of two separate single busbars without a tie breaker. All tie breakers are normally open besides the 11 kV main busbar system which is normally closed.

### 3.2 | Transformers

There are four *stand-alone* transformers on the platform. In this context, stand-alone means that they directly connect two busbar systems of different voltage in contrast to the other converter transformers that are dedicated to connecting a power electronic converter.

- The two larger units supply electricity from the 11 kV main busbar system to the 690 V utility busbar system. These transformers have a rating of 3.3 MVA each, a short circuit voltage of 11 %, with 0.35 % losses. They have delta windings on the high voltage side and star windings at the low voltage side, with the star point earthed with a 4  $\Omega$  resistor (100 A)
- The two smaller units supply the accommodation facilities at 400 V from the 690 V utility busbar system. These transformers have a rating of 600 kVA each, a short circuit voltage of 6%, with 1% losses. They have a similar delta-star configuration, but their star point is directly earthed.

### 3.3 | Cables

Three AC cable types and one DC cable type are used on the platform:

- 33 kV  $3 \times 240 \text{ mm}^2$  XLPE-insulation copper-conductor AC cables are used for the wind turbines. This cable type has a rated current of 489 A.
- 11 kV  $3 \times 120 \text{ mm}^2$  XLPE-insulation copper-conductor AC cables are used for the majority of applications. This cable type has a rated current of 360 A.
- 11 kV  $3 \times 240 \text{ mm}^2$  XLPE-insulation copper-conductor AC cables are used where a higher current rating of 520 A is needed. For the connection of each gas turbine generator, four parallel cables of this type are used. This cable type is (for simplicity) also used for the two short low voltage connections between the 690 V busbar system and the 690–400 V transformer at the accommodation facilities (even though a lower voltage rating would be sufficient there).
- 1.5 kV<sub>DC</sub>  $1 \times 500 \text{ mm}^2$  XLPE-insulation copper-conductor DC cables are used for the connection between the drilling DC busbar system and the rectifiers that feed power to it. Four cables in parallel are used for each connection, due to the high currents involved.

### 3.4 | Gas turbine generators

The platform has four gas turbine generators with a rated power of 28 MVA, rated voltage of 11 kV and rated power

factor of 0.85. One of these is normally not in use. They have star windings, and the star point is earthed with 127  $\Omega$  (50 A). The generators are directly connected to the main busbar system. The gas turbines are controlled by governors and the synchronous generators by static excitation systems. All turbine-generator-transformer setups are identical.

### 3.5 | Wind turbine generators

The gasturbine-based electricity supply of the LEOGO platform is accompanied by three 8 MW direct drive type-4 wind turbines. The rated power factor is 0.9, and the generator voltage is 690 V, which is transformed to 33 kV by a dedicated transformer. The wind turbine model attempts to resemble the Siemens Gamesa SG 8.0–167 DD wind turbine, as this turbine type is used for the same purpose on a real offshore installation (the Hywind Tampen project [22]). However, as no model of the SG 8.0–167 DD is openly available, the similarity is limited to the general parameters like power rating, turbine type, voltage level, power curve etc. The details of the implemented wind turbine model just resemble a generic wind turbine.

### 3.6 | Induction motors

There are three types of directly grid-connected induction motors:

- Three sea water lift pumps (SWL) are driven by 750 kW 11 kV induction motors with a rated power factor of 0.87 and an efficiency of 96.9 %
- Two air compressors (ACO) are driven by 1.3 MW 11 kV induction motors with a rated power factor of 0.9 and an efficiency of 95.9 %
- Two induction motors (ASM) at 0.25 MW and 690 V with a rated power factor of 0.92 and an efficiency of 96.1 %, generally representing one of the low voltage machines at the utility busbars.

All induction motors that are a part of a variable speed drive are not modelled in detail, as explained in Subsection 3.7.

### 3.7 | Variable speed drives

The *regular* (with dedicated power supply) variable speed drives (VSDs) consist of induction motors that are interfaced with a transformer and a back-to back AC-DC-AC converter. The transformer is not earthed and draws electric power from the main 11 kV busbar and reduces the voltage to a suitable level for the drive. This reduced AC voltage is then rectified by the active grid-side converter to provide the AC-DC-AC converters an internal DC voltage. The machine-side converter is supplied from this internal DC voltage, and it drives the machine with a variable frequency and variable voltage AC.

There are three types of variable speed drives:

- 10 MW is the rating of the largest VSDs. Their transformer is delivering 3.3 kV from the main 11 kV busbar, and this is then rectified to +6 kV<sub>DC</sub> by the active grid side converter
- 4.8 MW is the rating of the medium-size VSDs. They operate at the same voltage levels as the 10 MW units, just at lower currents.
- 1.5 MW is the rating of the smaller VSDs. Their transformer delivers 690 V<sub>AC</sub> from the main 11 kV busbar. This 690 V<sub>AC</sub> is then rectified to +1300 V<sub>DC</sub> by the active grid side converter.

In addition to these *regular* VSDs, there are the drilling VSDs that share a common power supply. There are two parallel transformer-converter systems where the 3.3 MVA transformer (not earthed) draws power from the 11 kV busbar, transforms it to 690 V, and the active power converter rectifies it, and supplies the +1300 V<sub>DC</sub> busbar system, as mentioned in Subsection 3.1. This common DC busbar is different as compared to the other VSDs, where the DC voltage is only internal to each back-to-back converter. The machine side converters of the drilling VSDs are supplied from the common DC busbar, and they drive the induction machines.

For all VSDs, the induction machine and the machine-side converter are not yet modelled in detail; they only appear as an ideal DC loads, which is how they behave as seen from the grid in a steady-state operation. This simplification was judged acceptable, as the back-to-back converter setup of the VSDs sufficiently decouples the grid dynamics from the rotating machine. It is, however, planned to improve the model in the future by adding these details.

### 3.8 | General low voltage loads

All the smaller loads (less than 250 kVA) are not modelled one by one in detail, but represented as aggregated loads. There are two types of these aggregated loads:

- Two 690 V<sub>AC</sub> loads at the utility busbars with a rating of 2.75 MW and an actual consumption of 1.05 MW, and a power factor of 0.9. 60% of this load is induction motors, while the remaining 40% are static frequency-independent loads with the composition of 28% constant power, 4% constant current and 8% constant resistance.
- Two 400 V<sub>AC</sub> loads at the accommodation busbars with a rating of 0.5 MW and an actual consumption of 0.25 MW, and a power factor of 0.98. About 10% of this load is induction motors, while the remaining 90% are static frequency-independent loads with the composition of 36% constant power, 9% constant current and 45% constant resistance.

## 4 | EXAMPLES OF SIMULATION RESULTS

Simulation results from both the operational optimisation model and the electrical model are presented in this section. The purpose of this is not the results in itself, but to demonstrate that the LEOGO platform specification makes sense and delivers reasonable results.

### 4.1 | Operational optimisation model

The platform specification above has been implemented as an input dataset [2] for analyses with the openly available Oogeso tool [23]. The system as represented in Oogeso is illustrated in Figure 6. As shown in the figure, the emphasis is on the energy system, with a rather simplified description of the processing. For example, the separation process is represented by a single unit, and the multi-phase wellstream flow is represented by its oil, gas and water components.

The main reason for including the processing system is to capture the link between energy demand and oil and gas production and its main constraints. This will be relevant when considering the potential for demand-side flexibility to allow higher share of wind energy supply with minimum energy storage requirements.

The Oogeso tool applies a rolling horizon mixed-integer linear optimisation model to schedule the generation output and start and stop signals based on forecasts of demand and energy availability. The rolling horizon is to account for delays in ramping and flexibility in storage utilisation or demand. The objective in this optimisation is to maximise the revenue, which means to keep the oil and gas export at maximum while minimising the cost of power generation. This favours wind before gas turbines. For gas turbines, there is a cost for starting up and a starting time of 30 min. The startup cost penalises shutdown and restart within the 2 h horizon being optimised, but as seen in the results below, it does not prevent multiple starts and stops within a single day. CO<sub>2</sub> emissions are computed from the fuel consumption curves for gas turbines (Figure 3) and the assumed CO<sub>2</sub> content of natural gas (Table 1).

To demonstrate that the LEOGO specification makes sense, two simple simulations have been run over a timespan of 1000 min with timesteps of 5 min. The first is a modified version of the base case (see Table 3), where the wellstream flow is reduced by 25% between the 500 and 750 min points. The second simulation represents Variation A and includes wind turbines with their associated variability.

Figure 7 shows the supply by source in the two simulation cases. The observed small fluctuations in total power demand and supply are due to the small variations in the input wellstream flow rate data. In the base case, we see that initially all three gas turbines are online, sharing the load evenly. As the wellstream flow drops after 500 min, the energy demand in

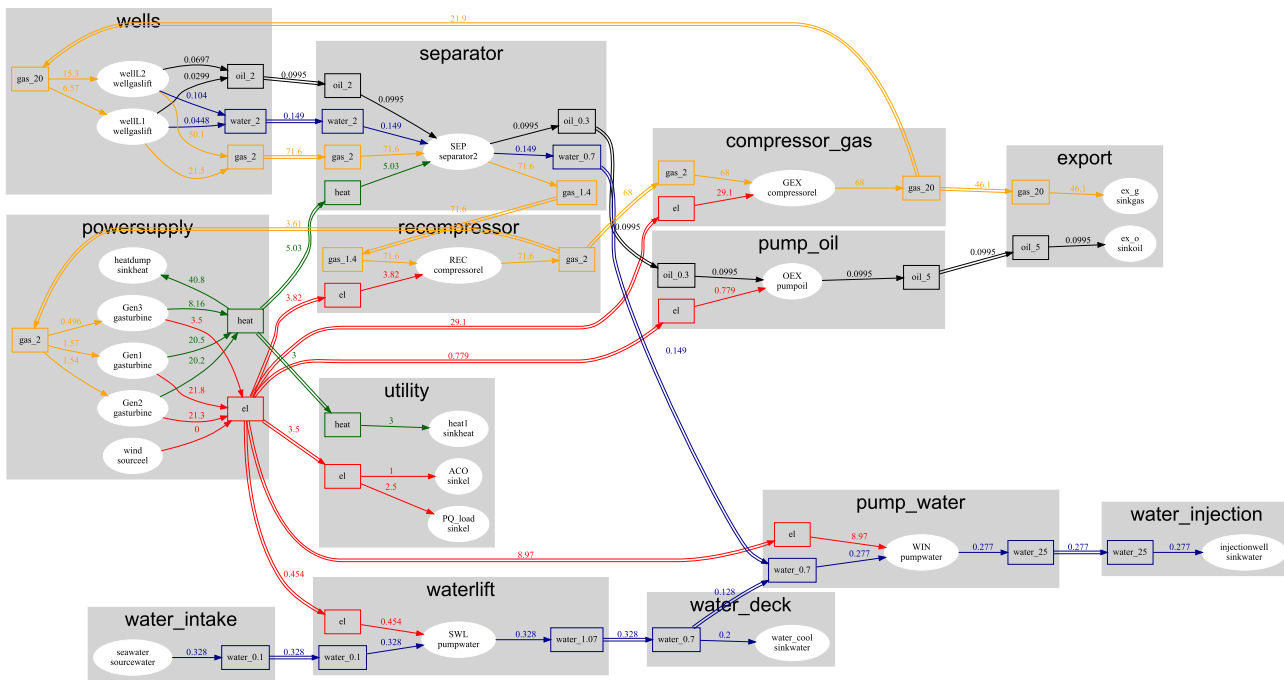


**FIGURE 6** Overview of the LEGO model represented in Oogeso. Edge colours represent different energy carriers, and the numbers indicate the flow ( $\text{Sm}^3/\text{s}$  or MW). The numbers in the square boxes indicate the inlet/outlet pressure levels (MPa).

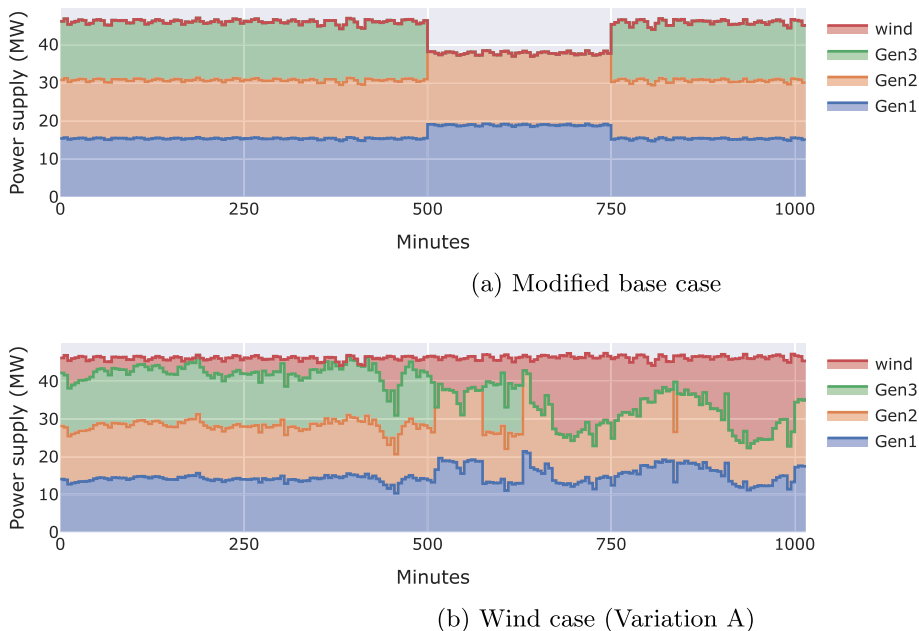


**FIGURE 7** Power supply from each generator in the two simulation cases.

compressors and pumps also drops and then only two gas turbines are needed. Switching off the third generator is beneficial because the efficiency of the gas turbines is higher at higher loading, resulting in lower total fuel consumption and therefore lower  $\text{CO}_2$  emissions per output electric power. In the case with wind power, there is more variability in gas turbine output and multiple start and stops of the third gas turbine to compensate for the variable wind. In this example,

the full costs of gas turbine starts and stops, related to wear and tear, is not captured, leading to unrealistically frequent starts and stops. This should be improved in more detailed future analyses.

The available online power reserve is shown in Figure 8. In the base case, there is plenty of available reserve when all three gas turbines are running. When the power demand drops after 500 min, the third gas turbine is switched off, as the two

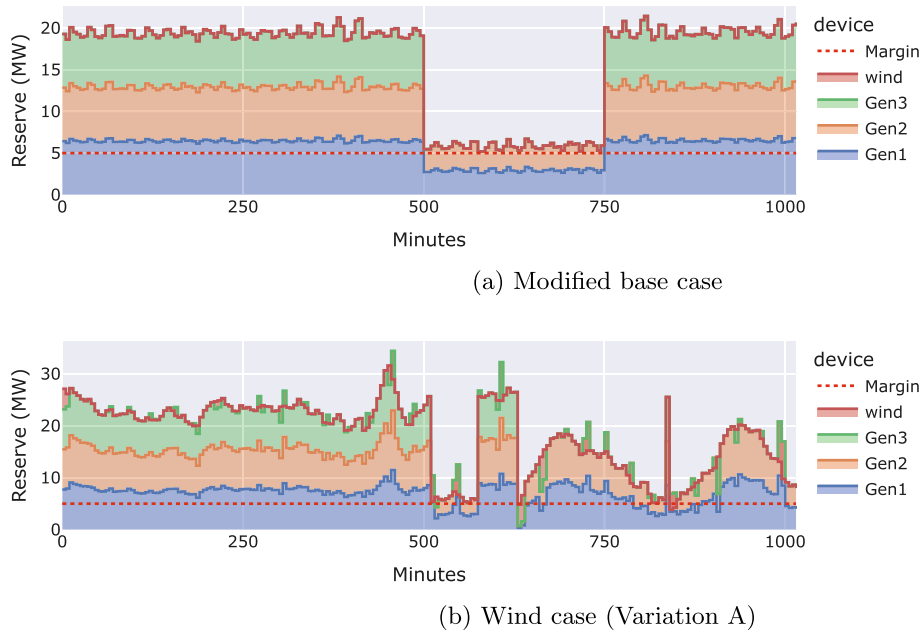


FIGURE 8 Online reserve provided by each generator in the two simulation cases.

remaining gas turbines are then sufficient to both cover the load and provide the required reserve. At 750 min, the power demand increases and then the third gas turbine is switched on again. Although two gas turbines could still provide sufficient power to meet the demand, there would not be enough reserve without the third gas turbine.

In the case with wind power, we see a similar situation with plenty of available reserve when all three gas turbines are on and the operation close to the threshold otherwise.

A thorough analysis of different configurations and operating strategies of the LEOGO platform is planned for a separate publication.

## 4.2 | Electrical model

The electrical system (more precisely, the electro-mechanical system), as described in Section 3, has been implemented in the DIGSILENT PowerFactory simulation tool. As this model contains no proprietary information, it has been made public and can be freely downloaded [2], used and modified. This RMS domain model is suitable to assess the electrical system behaviour in more detail, allowing to study the power flow, electro-mechanical transients, outer-level controls, stability indices etc.

The electrical model and the operational optimisation model are not interlinked, as they are meant to operate on different time scales. This means that any change in energy consumption or production identified by the operational model will not automatically make changes in the electrical model. However, any operational state from the operational model can be (manually) implemented in the electrical model by adjusting the set points.

To display some of the functionalities of the model, the event of the loss (disconnection) of a gas turbine has been simulated for the base case (three gas turbines only) and the Variation A (three gas turbines and three wind turbines). The battery of Variation B has not yet been implemented in the electrical model.

In the base case, wind power output is zero, and all three gas turbines operate each at 16.1 MW). In Variation A, the three wind turbines operate in a synthetic turbulent wind field that resembles a 'typical' situation in the North Sea. The wind power infeed into the main bus bar is (at the moment of the incident) 10.8 MW, which represents the sum of the three wind turbine outputs minus losses of the wind power collection system. It should, however, be remembered that wind fluctuations are basically irrelevant (0.1 MW) in the context of the severe incident simulated on a short 5 s time window as shown in the figure. The three gas turbines deliver each 12.4 MW.

The disconnection of a gas turbine is a critical event that stresses the electrical power system beyond the capability of the 5 MW operational reserve. To cope with the incident, 200 ms after the loss of gas turbine 3, all three water injection pumps (3 MW each) are stopped by the load shedding system in order to help restore the power balance. This reaction has been implemented manually, as the LEOGO electrical model does not have a load shedding system implemented in the software.

The frequency course during the simulated events is displayed in Figure 9, and the active power output of the gas turbine one is displayed in Figure 10.

In the zero-wind-power simulation (black curves), 16.1 MW of generation is lost, and this initial power shortage is drawn from the rotational inertia of the directly grid-connected rotating electrical machines (mostly the gas turbine generators),

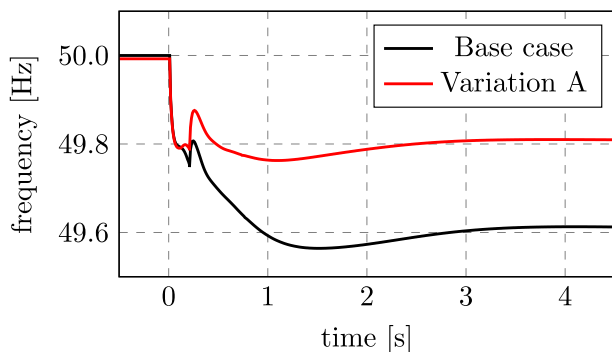


FIGURE 9 Electrical frequency at the main busbar.

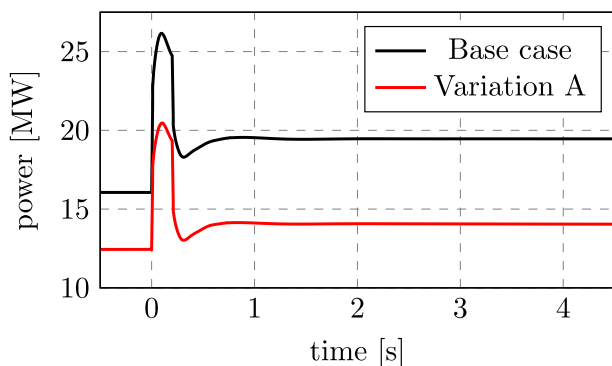


FIGURE 10 Active power output of gas turbine 1.

leading to a fast decline of the grid frequency. The resulting shedding of 9 MW load significantly relieves the situation, slowing down the frequency decline. Finally the turbine governors increase the gas turbine power output, re-establishing the power balance at a new operating point (19.5 MW) at around 49.6 Hz. A small part of the imbalance is covered by a consumption reduction due to frequency-dependency of the load.

In the Variation A simulation (red curves), the power imbalance is smaller, as the lost gas turbine three was operating at a lower power (12.4 MW). The initial transient is similar, but the load shedding (still 9 MW) relieves most of the imbalance. The needed power output increase of the remaining gas turbines is therefore smaller, and the new operating point is reached at 14.1 MW at around 49.8 Hz. Also here is a small part of the imbalance covered by a consumption reduction.

Both events lead to a significant frequency disturbance, which is accompanied by some decaying electro-mechanical oscillations. The simulations show the electro-mechanical transients in case of a major power imbalance as an example of what such an electro-mechanical RMS-domain model can simulate.

It should be noted that all of the simulations were performed with a *standard* wind turbine controller. This means operation at maximum power without upward headroom and no response to the frequency disturbance with supportive control actions like fast frequency support or virtual inertia,

which could assist the remaining gas turbines in handling the incident.

## 5 | CONCLUSION

This article has presented the LEOGO platform as an open reference case that can be easily shared and where no data are confidential. Its main purpose is to make it easy to investigate and compare the operation of low-emission oil and gas platform energy systems or more general off-grid energy systems to test modelling concepts, operational planning strategies, control implementations etc. in a transparent way. It facilitates comparisons of results obtained using different approaches and makes it easier for modellers to benefit from each other, which is the case for studies where the underlying assumptions and data are confidential or poorly documented.

The specification has a strong emphasis on the energy system, and more comprehensive descriptions of the fluid transport and processing systems are left for potential future work. Also, a description of the reservoir would be a natural extension. The ongoing research is investigating processing system constraints and the links between flow rates and energy demand, with the aim to develop linearised models for investigating the potential for utilising energy system flexibility in combination with variable wind. Updates to the electrical model may be needed to perform more detailed electrical analyses, to investigate more advanced control strategies and to check the influence on stability. Details to be realised in future revisions include the machine-side power converters and the machines of the VSDs and a power management system that coordinates the operation of the gas turbines.

The LEOGO platform has been presented as an off-grid energy system, but grid-connected alternatives are also interesting and should be considered for future specifications of LEOGO *variations*. This may include high voltage AC or DC connections to the mainland grid and/or connections between multiple LEOGO-like platforms in an offshore cluster.

### 5.1 | Getting involved

The LEOGO platform specification and open data have been created to be a useful reference case for different types of studies by anyone interested. The Oogeso simulation tool [23] used in Section 4.1 includes LEOGO as an example case, and the Oogeso documentation is therefore a good starting place for anyone interested in integrated energy system analyses. For electrical analysis, the PowerFactory simulation model can be downloaded [2], and it can be modified and expanded upon as desired. To use it, the PowerFactory software is required.

It is inevitable that for many studies, the present specification will be insufficient. In this case, we hope that the LEOGO users fill the gaps and publish these so they can be included with future updates of LEOGO. Modifications of general interest may be included as well as LEOGO variations.

We encourage others to use, improve and modify this specification and share these changes together with the results.

## ACKNOWLEDGEMENTS

The work reported here has received financial support by the Research Council of Norway through PETROSENTER LowEmission (project code 296207). We would like thank our industry partners in the LowEmission centre for valuable feedback and input to the LEOGO specifications.

## CONFLICT OF INTEREST

The authors declare that there is no conflict of interest.

## DATA AVAILABILITY STATEMENT

The data that support the findings of this study are openly available in Zenodo at <https://doi.org/10.5281/zenodo.7373223>, reference number [2].

## ORCID

Harald G. Svendsen  <https://orcid.org/0000-0002-8882-4316>

## REFERENCES

- Roussanaly, S., et al.: Offshore power generation with carbon capture and storage to decarbonise mainland electricity and offshore oil and gas installations: a techno-economic analysis. *Appl. Energy*. 233-234, 478–494 (2019). <https://doi.org/10.1016/j.apenergy.2018.10.020>
- Svendsen, H.G., Holdyk, A., Vrana, T.K.: LEOGO Reference Platform Dataset v2.0 (2022). <https://doi.org/10.5281/zenodo.7373223>
- Korpås, M., et al.: A case-study on offshore wind power supply to oil and gas rigs. *Energy Proc.* 24, 18–26 (2012). <https://doi.org/10.1016/j.egypro.2012.06.082>
- Nguyen, T.-V., et al.: CO<sub>2</sub>-mitigation options for the offshore oil and gas sector. *Appl. Energy*. 161, 673–694 (2016). <https://doi.org/10.1016/j.apenergy.2015.09.088>
- Nguyen, T.-V., et al.: Energy efficiency measures for offshore oil and gas platforms. *Energy*. 117, 325–340 (2016). <https://doi.org/10.1016/j.energy.2016.03.061>
- Riboldi, L., Nord, L.O.: Offshore power plants integrating a wind farm: design optimisation and techno-economic assessment based on surrogate modelling. *Processes*. 6(12), 249 (2018). <https://doi.org/10.3390/pr6120249>
- Fard, R.N., Tedeschi, E.: Integration of distributed energy resources into offshore and subsea grids. *CPSS trans. power electron. appl.* 3(1), 36–45 (2018). <https://doi.org/10.24295/CPSSSTPEA.2018.00004>
- Riboldi, L., et al.: Optimal design of a hybrid energy system for the supply of clean and stable energy to offshore installations. *Front. Energy Res.* 8, 346 (2020). <https://doi.org/10.3389/fenrg.2020.607284>
- Norwegian Petroleum Directorate.: Open Data (2021). <https://www.npd.no/en/about-us/information-services/open-data/>. Accessed 17 Sept 2021
- Lie, K.-A.: An Introduction to Reservoir Simulation Using MATLAB/GNU Octave: User Guide for the MATLAB Reservoir Simulation Toolbox (MRST). Cambridge University Press, Cambridge (2019). <https://doi.org/10.1017/9781108591416>
- Bothamley, M.: Offshore processing options for oil platforms. In: 2004 SPE Annual Technical Conference and Exhibition (2004). <https://doi.org/10.2118/90325-MS>
- Nguyen, T.-V., et al.: Exergetic assessment of energy systems on north sea oil and gas platforms. *Energy*. 62, 23–36 (2013). <https://doi.org/10.1016/j.energy.2013.03.011>
- Nguyen, T.-V., et al.: On the definition of exergy efficiencies for petroleum systems: application to offshore oil and gas processing. *Energy*. 73, 264–281 (2014). <https://doi.org/10.1016/j.energy.2014.06.020>
- Nguyen, T.-V., et al.: Thermodynamic analysis of an upstream petroleum plant operated on a mature field. *Energy*. 68, 454–469 (2014). <https://doi.org/10.1016/j.energy.2014.02.040>
- Voldsund, M., et al.: Exergy destruction and losses on four north sea offshore platforms: a comparative study of the oil and gas processing plants. *Energy*. 74, 45–58 (2014). <https://doi.org/10.1016/j.energy.2014.02.080>
- Hadiya, M.: Case Study of Offshore Wind Farm Integration to Offshore Oil and Gas Platforms as an Isolated System – System Topologies, Steady State and Dynamic Aspects. Master's thesis, NTNU (2011). <http://hdl.handle.net/11250/257145>
- Sandmo, T.: The Norwegian Emission Inventory 2016. Technical Report Documents 2016/22, SSB (2016). <https://www.ssb.no/en/natur-og-miljo/artikler-og-publikasjoner/the-norwegian-emission-inventory-2016>. Accessed 17 Sept 2021
- Gonzalez-Salazar, M.A., Kirsten, T., Prchlik, L.: Review of the operational flexibility and emissions of gas- and coal-fired power plants in a future with growing renewables. *Renew. Sustain. Energy Rev.* 82, 1497–1513 (2018). <https://doi.org/10.1016/j.rser.2017.05.278>
- Wärtsilä: Combustion Engine vs Gas Turbine: Startup Time. <https://www.wartsila.com/energy/learn-more/technical-comparisons/combustion-engine-vs-gas-turbine-startup-time>. Accessed 17 Sept 2021
- Haglund, F., Elmegaard, B.: Methodologies for predicting the part-load performance of aero-derivative gas turbines. *Energy*. 34(10), 1484–1492 (2009). 11th Conference on Process Integration, Modelling and Optimisation for Energy Saving and Pollution Reduction. <https://doi.org/10.1016/j.energy.2009.06.042>
- Vegvesenet: Sulafjorden E39 Wind Mast Measurements. <https://www.vegvesen.no/Europaveg/e39sulafjorden/malinger>. Accessed 16 April 2021
- Equinor: Hywind Tampen (2021). <https://www.equinor.com/en/what-we-do/hywind-tampen.html>. Accessed 07 Feb 2021
- Svendsen, H.G., Aslesen, M.D.: Offshore Oil and Gas Energy System Operational Optimisation (Oogeso) Software Code v1.0.0. Zenodo. <https://doi.org/10.5281/zenodo.5971182>

**How to cite this article:** Svendsen, H.G., et al.: The Low Emission Oil and Gas Open reference platform—An off-grid energy system for renewable integration studies. *IET Energy Syst. Integr.* 1–14 (2022). <https://doi.org/10.1049/esi2.12085>